Available online at www.sciencedirect.com
SCIENCE DIRECT
Catalysis Today 111 (2006) 119–132
CATALYSIS TODAY
www.elsevier.com/locate/cattod

An overview of aqueous-phase catalytic processes for production of hydrogen and alkanes in a biorefinery

George W. Huber, James A. Dumesic *

Department of Chemical and Biological Engineering, University of Wisconsin, 1415 Engineering Drive, Madison, WI 53706, USA

Available online 16 November 2005

Abstract

In this overview we discuss how aqueous-phase catalytic processes can be used to convert biomass into hydrogen and alkanes ranging from C_1 to C_{15}. Hydrogen can be produced by aqueous-phase reforming (APR) of biomass-derived oxygenated hydrocarbons at low temperatures (423–538 K) in a single reactor over supported metal catalysts. Alkanes, ranging from C_1 to C_6 can be produced by aqueous-phase dehydration/hydrogenation (APD/H). This APD/H process involves a bi-functional pathway in which sorbitol (hydrogenated glucose) is repeatedly dehydrated by a solid acid (SiO_2–Al_2O_3) or a mineral acid (HCl) catalyst and then hydrogenated on a metal catalyst (Pt or Pd). Liquid alkanes ranging from C_7 to C_{15} can be produced from carbohydrates by combining the dehydration/hydrogenation process with an upstream aldol condensation step to form C–C bonds. In this case, the dehydration/hydrogenation step takes place over a bi-functional catalyst (4 wt.% Pt/SiO_2–Al_2O_3) containing acid and metal sites in a specially designed four-phase reactor employing an aqueous inlet stream containing the large water-soluble organic reactant, a hexadecane alkane sweep stream, and a H_2 inlet gas stream. The aqueous organic reactant become more hydrophobic during dehydration/hydrogenation, and the hexadecane sweep stream removes these species from the catalyst as valuable products before they go on further to form coke.

Keywords: Aqueous-phase reforming; Hydrogen production; Renewable energy; Fuel cells; Aqueous-phase processing; Bio-fuels

1. Introduction

Environmental and political problems created by our dependence on fossil fuels combined with diminishing petroleum resources are causing our society to search for new renewable sources of energy and chemicals, and it has been said that the only foreseeable source of sustainable organics fuels, chemicals and materials is plant biomass [1]. Fuels derived from biomass are greenhouse gas neutral, because any CO_2 produced during fuel combustion is consumed by further growth of biomass (neglecting CO_2 produced by combustion of fossil fuels in biomass production, transportation and conversion [2]). The Roadmap for Biomass Technologies [3], authored by 26 leading experts from academia, industry and government agencies, has predicted a gradual shift from a petroleum-based economy to a more carbohydrate-based economy, such that by 2030, 20% of transportation fuel and 25% of chemicals will be produced from biomass.

The current cost of delivered biomass on an energy basis is $20–36 per barrel of oil equivalent (boe) [4], which is below the current price of crude oil ($49 per barrel). (All prices in this article are quoted in terms of U.S. dollars.) Even cheaper costs of biomass, $5–25 per boe, have been reported by Lynd et al. [1]. Continued research is being conducted to develop dedicated biomass energy crops, which have significantly higher yields than current crops [4]. In addition, a large amount of low-cost (or even free) biomass is currently available in the U.S. as waste material, with an energy content of 15.1 EJ/yr (1 EJ = 10^{18} J) [4]. The U.S. consumes 41 EJ/yr of oil [5], and waste biomass could thus displace a large amount of oil, provided that efficient processes can be developed for conversion of waste biomass into liquid fuels. It has been estimated that the U.S. could produce 1.1 Pg (1 Pg = 10^{15} g) of dry biomass per year and still meet its food, feed and export demands [6]. This amount of biomass has the energy content of 3.8×10^9 barrels of oil [4], and the U.S. consumes 7×10^9 barrels of oil per year [5].

* Corresponding author. Tel.: +1 608 262 1095; fax: +1 608 262 5434.
E-mail address: dumesic@engr.wisc.edu (J.A. Dumesic).

0920-5861/$ – see front matter © 2005 Elsevier B.V. All rights reserved.
doi:10.1016/j.cattod.2005.10.010

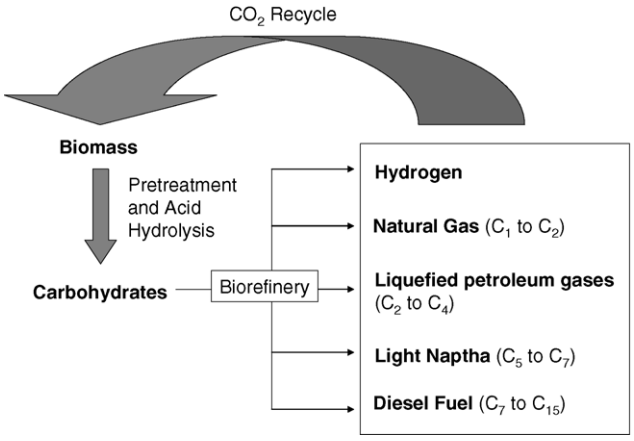

Fig. 1. An integrated biorefinery for conversion of carbohydrates to fuels by aqueous-phase processing.

While technologies have been developed over the past ~50 years to efficiently process petroleum-based feedstocks, we have not yet learned how to economically refine biomass resources. In this respect it has been stated that "the central and surmountable impediment to more widespread application of biocommodity engineering (or biorefining) is the general absence of low-cost processing technology" [1]. Despite the fact that heterogeneous catalysis has been the backbone of the chemical and petrochemical industry, few biorefining processes use heterogeneous catalysis. In this respect, the processing of biomass-derived feedstocks is different from the processing of petroleum-based feedstocks in that biomass-derived feedstocks have low thermal stability and a high degree of functionality (typically being hydrophilic in nature), thus requiring unique reaction conditions, such as aqueous-phase processing.

In this paper we discuss our recent work on aqueous-phase processing for conversion of biomass-derived oxygenates into hydrogen and alkanes (ranging from C_1 to C_{15}). These aqueous-phase processes could be used in an integrated biorefinery to produce a range of fuels, as shown in Fig. 1. The first step in the biorefining process is conversion of biomass into an aqueous sugar solution. Production of hydrogen for biorefining processes is accomplished by aqueous-phase reforming (APR) [7–17]. The biorefinery can also produce light alkanes ranging from C_1 to C_6 by aqueous-phase dehydration/hydrogenation (APD/H) [18]. The light alkanes could be used as synthetic natural gas, liquefied petroleum gas, and a light naptha stream. Aqueous-phase processing can also produce larger alkanes ranging from C_7 to C_{15} by combining the dehydration/hydrogenation reactions with an aldol condensation step prior to the APD/H step [19]. These larger alkanes could be used as premium, sulfur-free diesel fuel components.

2. Biomass

2.1. Chemistry of biomass

Plants capture solar energy as fixed carbon, from carbon dioxide and water in a sugar building block represented as $(CH_2O)_X$, as shown in Eq. (1). Typically 0.1–1.0% of the solar energy is captured with the biomass [4]. Plants have a variety of growth rates ranging from 0.6 to 16.4 kg/m^2 yr [4]. The sugar produced by photosynthesis is stored in a polymer form, which is a function of the type of plant material. This stored sugar is nature's building block for plants and the most abundant organic molecule on earth.

$$CO_2 + H_2O + \text{light} \underset{\text{chlorophyll}}{\longrightarrow} (CH_2O)_X + O_2 \quad (1)$$

Sugars in biomass are stored in three different types of polymers: starches, cellulose, or hemicellulose. Table 1 shows the chemical composition of representative types of biomass. Biomass is typically composed of 75–90 wt.% of sugar polymers, with the other 10–25 wt.% of biomass principally being large organic aromatic compounds called lignin [20]. Other components of biomass present in minor amounts include triglycerides, alkaloids, pigments, resins, sterols, terpenes, terpenoids, and waxes.

Cellulose, as shown in Fig. 2A, is a polysaccharide with a glucose monomer unit and β-1,4 glycoside linkages [21]. Cellulose has an average molecular weight range of 300,000–500,000, and it is the skeletal structure of most terrestrial biomass. Upon partial acid hydrolysis, cellulose can be broken down into cellobiose (glucose dimer), cellotriose (glucose trimer), and cellotetrose (glucose tetramer), whereas upon complete acid hydrolysis it is broken down into glucose. The β-1,4 glycoside linkages cause cellulose to be in a low surface area crystalline form.

Table 1
Chemical composition of representative biomass sources adapted from Klass [4]

Biomass type	Marine	Freshwater	Herbaceous	Woody	Woody	Woody
Name	Giant brown kelp	Water hyacinth	Bermuda grass	Poplar	Sycamore	Pine
Component (dry wt.%)						
Celluloses	4.8	16.2	31.7	41.3	44.7	40.4
Hemicelluloses		55.5	40.2	32.9	29.4	24.9
Lignins		6.1	4.1	25.6	25.5	34.5
Mannitol	18.7					
Algin	14.2					
Crude protein	15.9	12.3	12.3	2.1	1.7	0.7
Ash	45.8	22.4	5.0	1.0	0.8	0.5
Total	99.4	112.5	93.3	102.9	102.1	101.0

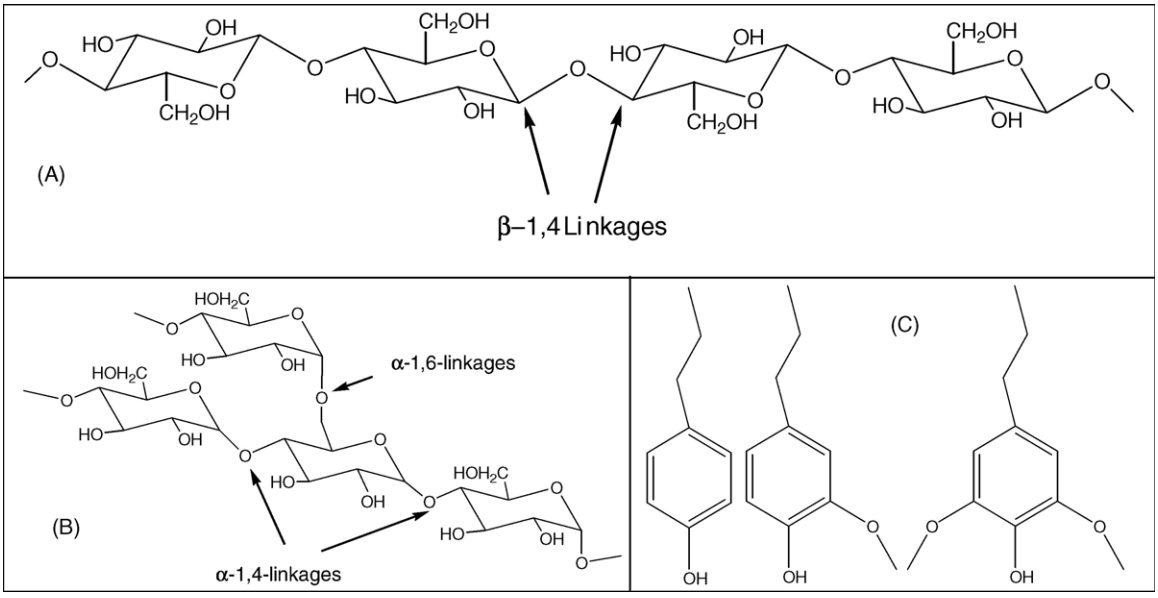

Fig. 2. Chemical structure of biomass derived compounds including: (A) cellulose with β-1,4 glucose linkages cellulose, (B) starches with α-1,4 and α-1,6 glucose linkages and (C) structural monomer units of lignin.

Starches are a polysaccharide of glucose, but in contrast to cellulose have α-1,4 glycoside linkages (Fig. 2B) [21]. Starches also contain a large amount of α-1,6 glycoside linkages. This polymer is highly amorphous because of the α-linkages, making it easy to be broken down into glucose by human and animal enzyme systems. Starches are commonly found in the vegetable kingdom (e.g., corn, rice, wheat, beans, potatoes). When treated in hot water, starches break down into two principle components: water soluble amylose (10–20%) and water insoluble amylopectin (80–90%). Amylose contains only α-1,4 glycoside linkages, whereas amylopectin contains both α-1,4 and α-1,6 glycoside linkages with an approximate α-1,4 to α-1,6 linkage ratio of 20 to 1, respectively.

Hemicellulose is a sugar polymer, which typically constitutes 20–40 wt.% of biomass [21]. In contrast to cellulose, which is a polymer of only glucose, hemicellulose is a polymer of five different sugars. This complex polysaccharide occurs in association with cellulose in the cell walls. It contains five-carbon sugars (usually xylose and arabinose), six-carbon sugars (galactose, glucose, and mannose), all of which are highly substituted with acetic acid. The most abundant building block of hemicellulose is xylan (a xylose polymer), which consists of xylose monomer units linked at the 1 and 4 positions. Hemicellulose is amorphous because of its branched nature, and relatively easy to hydrolyze to its monomer sugars compared to cellulose.

Biomass is usually composed of 10–25 wt.% lignin, consisting of highly branched, substituted, mononuclear aromatic polymers found in the cell walls of certain biomass, particularly woody biomass [21]. Fig. 2C shows some of the structural units of lignin [4]. Lignin is often associated with the cellulose and hemicellulose materials making up lignocellulose compounds.

Lignocellulose is one of the cheapest and most abundant forms of biomass, however, it is difficult to convert this unreactive material into sugars [22,23]. The crystalline portion of lignocellulose is composed of cellulose, whereas amorphous hemicellulose occurs in association with cellulose and lignin. Lignin makes up the walls of the lignocellulose material and must be broken down to make the cellulose or hemicellulose accessible to acid hydrolysis. Lignocellulose is difficult to convert to sugars because of the high crystallinity of the cellulose, low surface area of the material, protection of cellulose by lignin, the heterogeneous character of biomass particles, and cellulose sheathing by hemicellulose [23]. To convert lignocellulose to sugars, an effective pretreatment step must be employed to break the lignin seal and decrease the crystalline structure of the cellulose. Some of the pretreatment methods used for lignocellulose include: uncatalyzed steam explosion, treatment in liquid hot water or pH controlled hot water, flow through liquid hot water or dilute acid, flow-through acid, treatment with lime, and treatment with ammonia [23].

After suitable pretreatment, biomass can then be broken down into sugar monomers by acid or enzymatic hydrolysis. The National Renewable Energy Laboratory has estimated that the cost of unrefined sugar monomer solution from lignocellulose would be 12–14 ¢/kg_{sugar} [24]. Lynd et al. have estimated that projected technologies utilizing lignocellulosic feedstocks could decrease the price of sugars to as low as 5.3 ¢/kg [1].

2.2. Current processes for conversion of biomass to liquid fuels

Three main types of processes exist for production of liquid fuels from biomass, as shown in Fig. 3. These processes include gasification to produce syn-gas, thermochemical liquefaction and/or pyrolysis for bio-oils production, and acid hydrolysis for sugar production. These products are then further refined to produce: alkanes by Fischer–Tropsch synthesis from syn-gas, methanol by methanol synthesis from syn-gas [4], liquid alkane

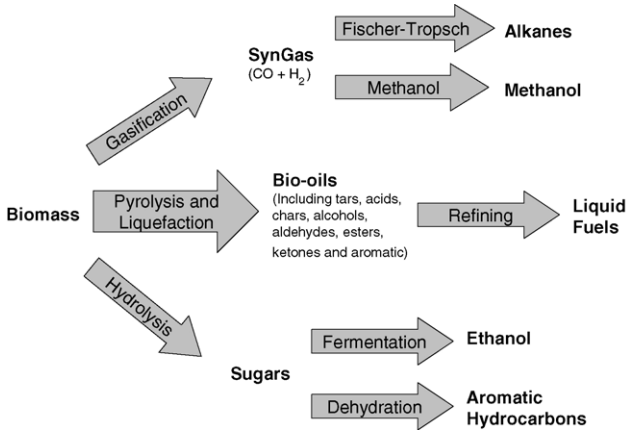

Fig. 3. Current strategies for production of liquid fuels from biomass.

fuels by upgrading products from liquefaction and pyrolysis [25,26], aromatic hydrocarbons (and coke) from conversion of sugars and methanol over zeolite catalysts [27,28], and ethanol production by fermentation of sugars. (The production of bio-diesel by esterification of triglycerides is also a major route to produce liquid fuels from biomass, but it is not discussed here because triglycerides comprise only a small fraction of biomass.)

At the present time, the production of ethanol by fermentation of carbohydrates is the primary technology for the generation of liquid fuels from renewable biomass resources. In 1998, the U.S. produced approximately 4.9×10^9 L of ethanol per year from starch-based biomass [20]. While not currently economically viable, research is being carried out to produce ethanol from more plentiful and inexpensive lignocellulose. The National Renewable Energy Laboratory has developed and modeled a process for conversion of corn stover (lignocellulose) to ethanol based on dilute acid prehydrolysis and enzymatic hydrolysis [24]. The feedstock cost for ethanol production from corn stover accounts for 31% of the total cost, with the other 69% of the cost coming from processing of the biomass [24].

Production of bio-oils by liquefaction or pyrolysis involves thermochemical treatment of biomass. An advantage of this process is that it is relatively simple, usually requiring only one reactor (thus having a low capital cost); however, this process is non-selective, producing a wide range of products including a large amount of char. Thermochemical treatment of biomass to produce hydrocarbons has been carried out since the 1930s in which Berl and co-workers showed that biomass could be converted to hydrocarbons by thermochemical treatments under basic conditions at 700 K [25,29,30]. These experiments led to a theory that oil was formed from biomass. After the hydrocarbons were formed they were then hydrogenated over a MoS_2 catalyst and separated based on their boiling points to gasoline, naptha, gas oil, heavy oil and asphalt. Typical products made from thermochemical processing of biomass include H_2, CO, CH_4, tars, acids, chars, alcohols, aldehydes, esters, ketones and aromatic compounds [4]. Research is currently being conducted to upgrade bio-oils to more valuable products [26].

Biomass can also be gasified to syn-gas (CO and H_2); however, the gasification process requires volatilization of water, decreasing the overall energy efficiency [31]. Syn-gas can be used to produce alkanes by Fischer–Tropsch synthesis (FTS), methane by methanation, methanol by methanol synthesis [32,33], and ethanol from fermentation [34]. The yield of diesel fuel from wood by FTS of biomass-derived syn-gas has been reported to be 120 $L_{dieselfuel}/Mg_{biomass}$ (1 Mg = 10^6 g) [35], which is lower than the yield of ethanol from wood which is reported to be 210 $L_{ethanol}/Mg_{wood}$ [4]; however, synthetic natural gas and electricity are also produced as by-products of FTS. Prins et al. have modeled the production of Fischer–Tropsch fuels from sawdust and have reported the overall energy efficiency (defined as energy in diesel fuel plus electricity divided by energy in biomass) to be 36% [36]. The major exergy losses (exergy is the amount of energy in a system that is able to do work) in a FTS plant as modeled by Prins et al. [36] are in the gasification, steam generation and power generation system.

Researchers at Mobil in the 1980s developed a process to produce aromatic hydrocarbons by passing carbohydrates over zeolite catalysts in the gas phase [27,28]. While this process is able to produce gasoline range hydrocarbons, approximately 40–50% of the carbon in the feed is converted to coke.

3. Hydrogen production by aqueous-phase reforming

3.1. Reaction mechanism

The catalytic pathway for the production of H_2 and CO_2 by aqueous-phase reforming (APR) of oxygenated hydrocarbons involves cleavage of C–C bonds as well as C–H and/or O–H bonds to form adsorbed species on the catalyst surface (Fig. 4). Cleavage of these bonds occurs readily over Group VIII metals, such as Pd and Rh [37]. Ethylene glycol and glycerol decompose on Pt to form adsorbed CO at room temperature [38,39]. Adsorbed CO species must be removed from the surface by the water-gas shift reaction to form CO_2 and H_2, because high surface coverages by CO lead to low catalytic activity.

Undesired byproducts may arise from parallel and series pathways (Fig. 4). Parallel reactions proceed via cleavage of C–O bonds followed by hydrogenation to give alcohols, or by rearrangement reactions to form organic acids. Series reactions arise from hydrogenation of adsorbed CO and CO_2 to form alkanes. Thus, a good catalyst for production of H_2 by APR must facilitate C–C bond cleavage and promote removal of adsorbed CO species by the water-gas shift reaction, but the catalyst must not facilitate C–O bond cleavage and hydrogenation of CO or CO_2.

A general reaction scheme for APR of ethylene glycol has previously been proposed for Pt/Al_2O_3 catalysts [13,14]. In this scheme, adsorbed ethylene glycol undergoes dehydrogenation on the surface followed by C–C bond cleavage and water-gas shift to give CO_2 and H_2 products. Adsorption of ethylene glycol, water, H_2 and CO_2 are assumed to be in quasi-equilibrium. Reaction kinetics measurements and FTIR studies have shown that the water-gas shift reaction is reversible, such that the ratio of the partial pressures of the products to the

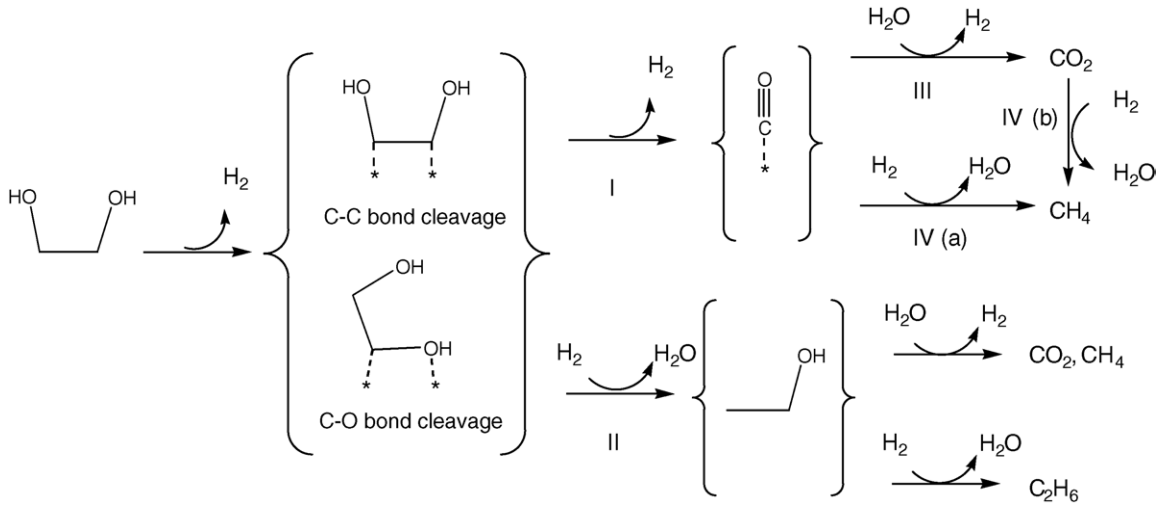

Fig. 4. Schematic representation of reaction pathways and selectivity challenges for production of H_2 from conversion of ethylene glycol with water. Pathway I is desired C–C cleavage to form adsorbed CO. Pathway II represents undesired C–O cleavage followed by hydrogenation to produce ethanol, leading to formation of methane and ethane. Pathway III is the desired water-gas shift reaction. Pathway IV represents undesired methanation and Fischer–Tropsch reactions to produce alkanes. (Figure adapted from [16].)

reactants divided by the water-gas shift equilibrium constant (i.e., $P_{H_2}P_{CO_2}/P_{CO}P_{H_2O}K_{eq}$) is higher than 0.5 [13,40]. In situ FTIR attenuated total reflectance (ATR) studies of APR for a 5 wt.% methanol solution at 423 K of a Pt/Al_2O_3 catalyst have shown that the surface coverage of CO is 35% while the surface coverage of CO for vapor phase reforming is 60% [13,40]. The rate of H_2 production is fractional order with respect to feed concentration (0.4 order) for APR of ethylene glycol with Pt/Al_2O_3 [13]. The rates of APR of methanol and ethylene glycol on Pt/Al_2O_3 catalysts are similar, indicating that the C–C bond cleavage is probably not the rate limiting step [13]. Reaction kinetics studies for APR of ethylene glycol with Pt/Al_2O_3 catalysts have shown that H_2 inhibits the rate of H_2 production (-0.7 order), indicating that adsorbed hydrogen atoms can block reaction sites under reaction conditions. Based on these results, two approaches to improve the catalytic activity of Pt-based catalysts can be suggested: (1) increase the rate for dehydrogenation of adsorbed ethylene glycol by alloying with a metal or metal oxide that has a higher rate of dehydrogenation or (2) increase the number of vacant Pt sites, perhaps by decreasing the heat of adsorption of strongly adsorbed species (e.g., CO^* and H^*) that block Pt sites under reaction conditions.

3.2. Catalyst development

3.2.1. Monometallic catalysts

A combination of high-throughput and fundamental studies were undertaken to develop catalysts for APR, as shown in Fig. 5. A high-throughput reactor was designed and built that allowed rapid screening of a large number of catalysts under APR conditions [11,12]. More than 500 different mono and bimetallic catalytic materials were screened using the high-throughput reactor, and inexpensive non-precious metal catalysts and highly active precious metal catalysts were identified. Promising catalysts were characterized and studied in more detail.

Reaction kinetic studies were conducted for the APR of ethylene glycol at low temperatures (483 and 498 K) and moderate pressures (22 bar) over silica-supported Ni, Pd, Pt, Ir, Ru and Rh catalysts. From our reaction kinetics studies, we found that the overall catalytic activity of APR of ethylene glycol (as measured by the rate of CO_2 production per surface site at 483 K) decreases in the following order for silica-supported metals [9]:

$$Pt \sim Ni > Ru > Rh \sim Pd > Ir$$

Silica-supported Rh, Ru and Ni catalysts showed low selectivity for production of H_2 and high selectivity for alkane production. In addition, Ni/SiO_2 showed significant deactivation at the higher temperature of 498 K. Thus, silica-supported Pt and Pd catalysts exhibited higher selectivity for production of H_2, with lower rates of alkane production.

The activity and selectivity of monometallic Pt-based catalysts can be improved further by supporting Pt on TiO_2, carbon, or Al_2O_3 [15]. The monometallic catalysts with the highest turnover frequencies for production of H_2 (TOF_{H_2}, sites counted by CO chemisorption) are Pt supported on TiO_2, carbon, and Al_2O_3 (i.e., 8–15 min^{-1} at 498 K for 10 wt.% ethylene glycol). Moderate catalytic activity for production of H_2 is demonstrated by Pt supported on SiO_2–Al_2O_3 and ZrO_2 (near 5 min^{-1}), and lower turnover frequencies are exhibited by Pt supported on CeO_2, ZnO, and SiO_2 (lower than about 2 min^{-1}). Catalysts consisting of Pt supported on carbon, TiO_2, SiO_2–Al_2O_3 and Pt-black also lead to the production (about 1–3 min^{-1}) of gaseous alkanes and liquid-phase compounds that would lead to alkanes at higher conversions (e.g., ethanol, acetic acid, acetaldehyde).

3.2.2. Bimetallic Pt and Pd catalysts

The activity of Pt catalysts can be improved further by adding Ni, Co or Fe to a Pt/Al_2O_3 catalyst [11]. Alumina-supported PtNi and PtCo catalysts with Pt:Co or Pt:Ni atomic

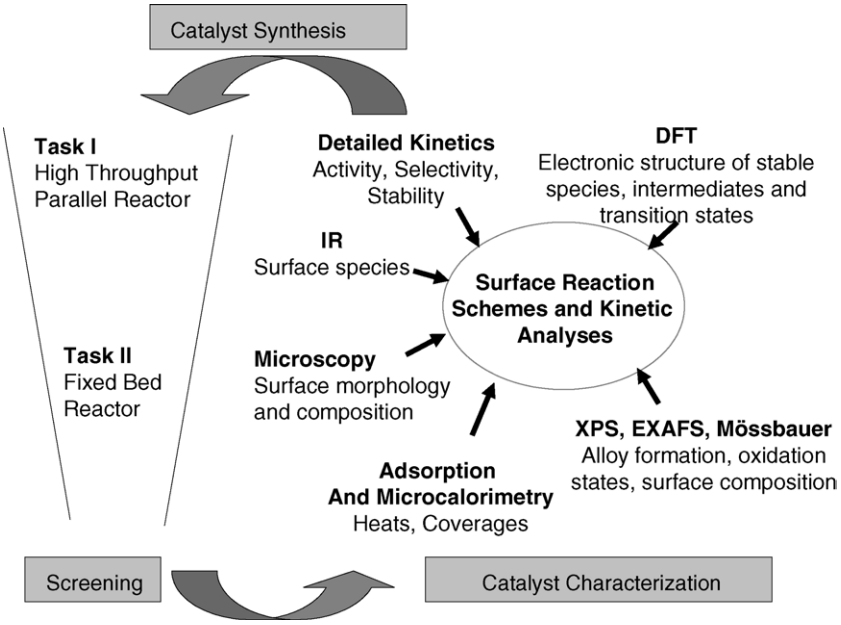

Fig. 5. Catalyst development philosophy.

ratios ranging from 1:1 to 1:9 had TOF_{H_2} values of 2.8–5.2 min^{-1} for APR of ethylene glycol solutions at 483 K, compared to a value of 1.9 min^{-1} for Pt/Al_2O_3 under similar reaction conditions. The $PtNi/Al_2O_3$ and $PtCo/Al_2O_3$ catalysts at 483 K were 2.1–3.5 times more active than the Pt catalyst per gram of catalyst. A Pt_1Fe_9/Al_2O_3 catalyst showed H_2 turnover frequencies of 0.3–4.3 min^{-1} at 453–483 K, and these values are about three times higher than Pt/Al_2O_3 under identical reaction conditions.

While Pd is the most selective monometallic catalyst, it has low activity for APR [11]. However, the activity of Pd can be increased by adding Fe to the catalyst. A Pd_1Fe_9/Al_2O_3 catalyst had values of TOF_{H_2} equal to 1.4 and 4.3 min^{-1} at temperatures of 453 and 483 K, respectively, and these values are 39–46 times higher than Pd/Al_2O_3 at the same reaction conditions. A catalyst consisting of Pd supported on high surface area Fe_2O_3 (Nanocat) had the highest intrinsic activity of any catalyst tested with values of TOF_{H_2} equal to 14.6, 39.1 and 60.1 min^{-1} at temperatures of 453, 483, and 498 K, respectively.

We suggest that alloying Pt with Ni, Co or Fe improves the activity for H_2 production by lowering the d-band center [41–44], which causes a decrease in the heats of CO and H_2 adsorption, thereby increasing the fraction of the surface available for reaction with ethylene glycol. It appears that the rate limiting step for APR of ethylene glycol on Pd-based catalysts is the water-gas shift reaction, and adding a water-gas shift promoter like Fe_2O_3 to Pd can improve the catalytic activity for APR. In general, bimetallic catalysts can have a significantly higher activity than monometallic catalysts for APR of ethylene glycol.

3.2.3. Bimetallic Ni–Sn catalysts

While Ni-based catalysts are active for APR, they have poor selectivity and stability for the APR reaction. The H_2 selectivity of Ni-based catalysts can be improved by adding Sn to the Ni catalyst, and the stability of Ni catalysts can be improved by using a bulk Ni catalyst [12,17]. A Raney-NiSn catalyst can be used to achieve good activity, selectivity, and stability for production of H_2 by APR of biomass-derived oxygenated hydrocarbons. This inexpensive material has catalytic properties that are comparable to those of Pt/Al_2O_3 for production of H_2 from small oxygenates, such as ethylene glycol, glycerol, and sorbitol. Rates of H_2 production by APR of ethylene glycol over R-NiSn catalysts with NiSn atomic ratios of up to 14:1 are comparable to 3 wt.% Pt/Al_2O_3, based on reactor volume.

The addition of Sn to Raney-Ni catalysts significantly decreases the rate of methane formation from series reactions of CO or CO_2 with H_2, while maintaining high rates of C–C cleavage necessary for production of H_2. However, it is necessary to operate the reactor near the bubble-point pressure of the feed and moderate space times to achieve high selectivities for production of H_2 over R-NiSn catalysts, while it is impossible to achieve these high selectivities under any conditions over unpromoted R-Ni catalysts. The Sn-promoted Raney-Ni catalyst is catalytically stable for more than 250 h time on stream [17].

4. Production of light alkanes by aqueous-phase dehydration/hydrogenation

4.1. Reaction mechanism

Aqueous-phase processing can be modified to selectively produce alkanes from sorbitol by increasing the acidity of the catalyst [18]. In this way, hexane can be produced by aqueous-phase dehydration/hydrogenation (APD/H) of sorbitol (Eq. (2)) with a catalyst containing metal (e.g., Pt or Pd) and acid (e.g., SiO_2–Al_2O_3) sites to catalyze dehydration and hydrogenation

reactions, respectively. Hydrogen for this reaction can be produced from APR of sorbitol (Eq. (3)) in the same reactor or in a separate reactor. The net reaction (Eq. (4)) is exothermic, in which approximately 1.5 mol of sorbitol produce 1 mol of hexane. The APD/H process occurs in the liquid phase, thereby eliminating the need to vaporize the aqueous feedstock and improving the overall thermal efficiency of the process. The alkanes produced, according to Eq. (4), retain approximately 95% of the heating value and only 30% of the mass of the biomass-derived reactant

$$C_6O_6H_{14} + 6H_2 \rightarrow C_6H_{14} + 6H_2O \quad (2)$$

$$C_6O_6H_{14} + 6H_2O \rightarrow 6CO_2 + 13H_2 \quad (3)$$

$$\frac{19}{13}C_6O_6H_{14} \rightarrow C_6H_{14} + \frac{36}{13}CO_2 + \frac{42}{13}H_2O \quad (4)$$

Fig. 6 shows the essential features of the bi-functional reaction scheme for production of alkanes from sorbitol. Hydrogen is produced on the metal by cleavage of C–C bonds followed by the water-gas shift reaction. Dehydrated species such as ring compounds (e.g., isosorbide) or enolic species are formed on acid sites [45], which migrate to metal sites where they undergo hydrogenation reactions. Repeated cycling of dehydration and hydrogenation reactions in the presence of H_2 leads to heavier alkanes (such as hexane) from sorbitol. Formation of lighter alkanes takes place by cleavage of C–C bonds compared to hydrogenation of dehydrated reaction intermediates. Lighter alkanes can also be formed by hydrogenation of CO and/or CO_2 on metals such as Ni and Ru [9].

The selectivities for production of various alkanes by APR depend on the relative rates of C–C bond cleavage, dehydration and hydrogenation reactions. The selectivities for production of alkanes can be varied by changing the catalyst composition, the reaction conditions, and modifying the reactor design [18]. In addition, these selectivities can be modified by co-feeding H_2 with the aqueous sorbitol feed, leading to a process in which sorbitol can be converted to alkanes and water without the formation of CO_2 (since H_2 is supplied externally and need not be produced as an intermediate in the process). As another variation, the production of alkanes can be accomplished by replacing the solid acid with a mineral acid (such as HCl) that is co-fed with the aqueous sorbitol reactant.

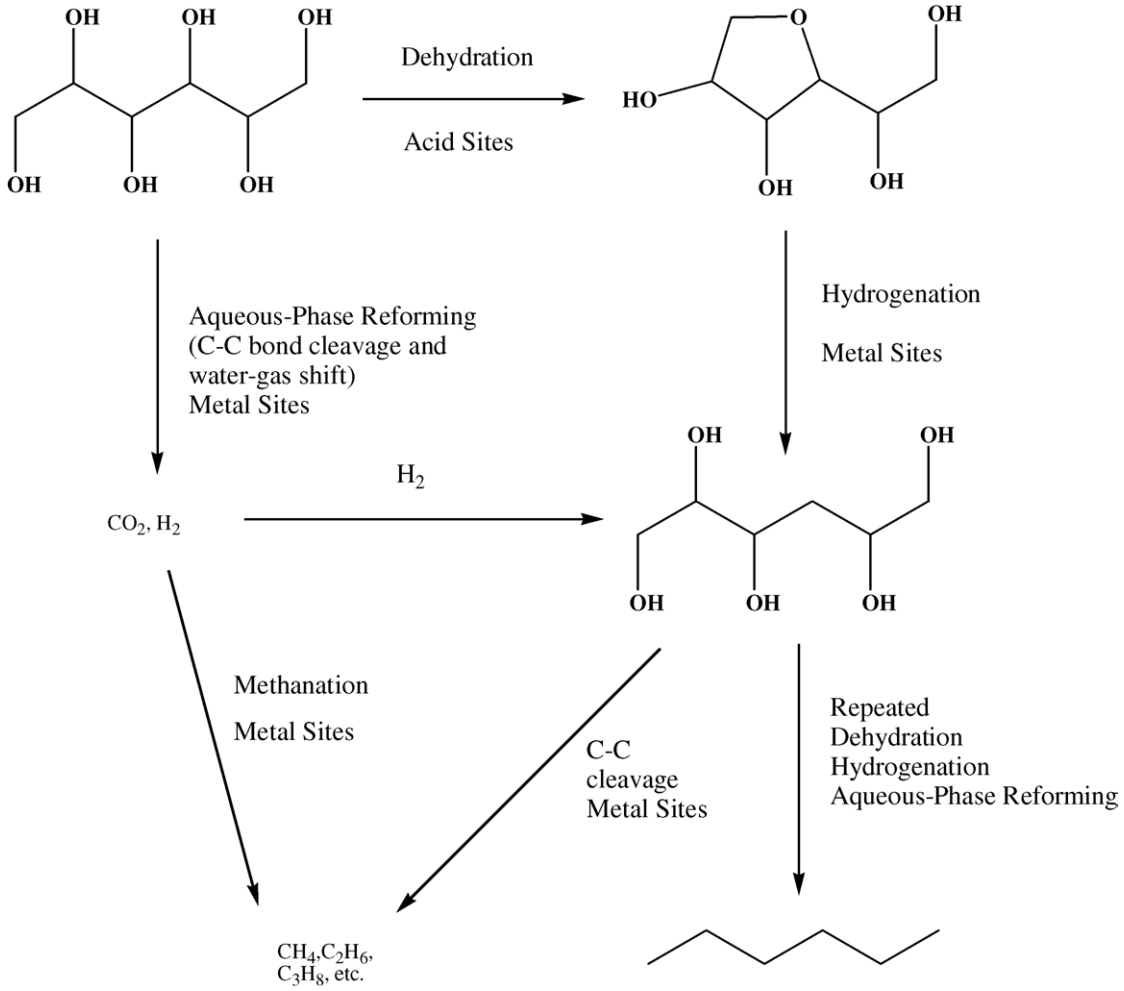

Fig. 6. Reaction pathways for production of alkanes from sorbitol over catalysts with metal and acidic components. (Figure adapted from [18].)

4.2. Bifunctional catalysts

Fig. 7A shows the carbon selectivity for APR of a 5 wt.% sorbitol feed with a Pt/Al_2O_3 catalyst, which is one of the best catalysts for H_2 production by APR. It should be noted that this carbon selectivity only takes into account the carbon in the alkanes, and CO_2 and H_2 are also being produced in this reaction. As observed from Fig. 7A, the selectivity to heavier alkanes increases for the non-acidic Pt/Al_2O_3 catalyst when the pH of the aqueous sorbitol feed is lowered by addition of HCl. The selectivity also shifts to heavier alkanes as more solid acid sites are added to a Pt/Al_2O_3 catalyst by physically mixing Pt/Al_2O_3 with SiO_2/Al_2O_3, as shown in Fig. 7B. Importantly, the H_2 selectivity decreases from 43 to 6% as the pH decreases from 7 to 2, indicating that the H_2 produced by APR (Eq. (3)) is consumed in alkane production (Eq. (2)). Similarly, the H_2 selectivity decreases from 43 to 11% as the solid acidity increases. Thus, alkanes are formed by a combination of metal and acidic components, since they are formed in only small amounts on the Pt/Al_2O_3 catalyst. The alkanes formed are straight-chain compounds with only minor amounts of branched isomers (less than 5%). Alkanes heavier than hexane were not formed under the reaction conditions of this study.

Platinum can also be added directly to the SiO_2/Al_2O_3. Fig. 8 shows the effect of temperature and co-feeding H_2 on the carbon selectivity for APD/H of 5 wt.% sorbitol over the 4 wt.% Pt/SiO_2–Al_2O_3 catalyst. No major difference is observed in the alkane distribution as the temperature is increased from 498 to 538 K (Fig. 8). The carbon selectivities for the Pt/SiO_2–Al_2O_3 catalyst and the physical mixture of Pt/Al_2O_3 with SiO_2–Al_2O_3 were similar, indicating that the Pt sites do not need to be in close contact with the acid sites. The selectivity for production of hexane increases when H_2 is co-fed with the aqueous sorbitol stream. Thus, increasing the H_2 partial pressure in the reactor increases the rate of hydrogenation compared to C–C bond cleavage on the metal catalyst surface. When H_2 was co-fed to the reactor, the carbon alkane selectivity (percent of carbon in the alkane products) was 91%, with the other 9% of the carbon leaving the reactor as CO_2. Importantly, all of the carbon entering the reactor was accounted for in the gas and liquid effluent streams, indicating

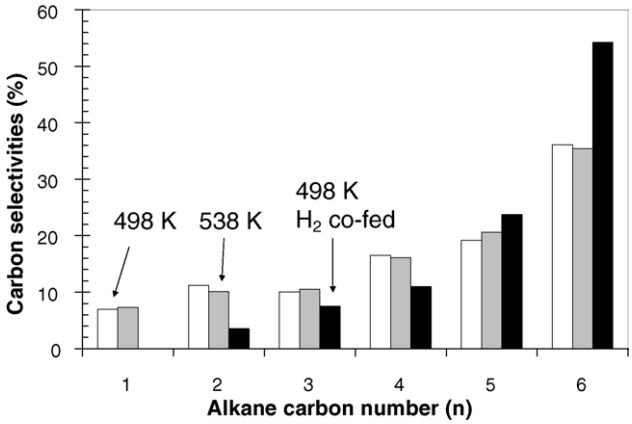

Fig. 8. Carbon selectivities for aqueous-phase dehydration/hydrogenation of 5 wt.% sorbitol over a 4 wt.% Pt/SiO_2–Al_2O_3. [Key: 498 K and 34.8 bar (white), 538 K and 60.7 bar (grey), and co-feeding H_2 at 498 K and 34.8 bar (black). Figure adapted from [18].]

that negligible amounts of coke were deposited on the catalyst surface. The Pt/SiO_2–Al_2O_3 catalyst did not exhibit deactivation over 2 weeks time-on stream.

4.3. Energy balance for production of alkanes

Fig. 9 shows the energy balance for conversion of glucose and H_2 to hexane, compared to the direct combustion of these compounds [46]. The conversion of glucose and H_2 to hexane is an exothermic reaction, which liberates 380 kJ/mol. The combustion of hexane liberates 3900 kJ/mol, which is approximately 90% of the energy that would be released if the glucose and H_2 feedstocks were combusted. Thus, the energy content of the liquid alkane fuel represents 90% of the energy content of the carbohydrate and the H_2 reactants. The conversion of carbohydrates to liquid alkanes involves the storage of a considerable amount of H_2 in the fuel (i.e., essentially 1 molecule of H_2 is used to convert each carbon atom in the carbohydrate reactant to an alkane moiety). The hexane contains 16 wt.% H, and glucose is thus an effective and energy efficient way to store H_2, because the infrastructure for using and distributing liquid fuels is already in place. Hydrogen

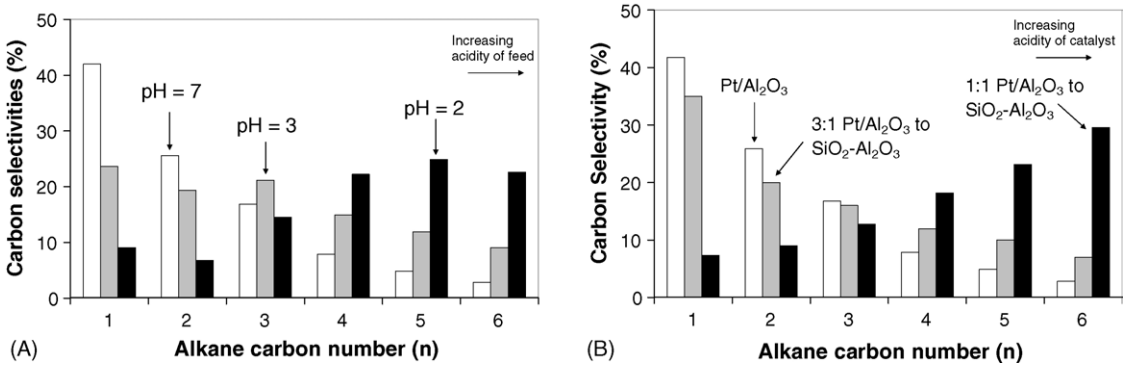

Fig. 7. Carbon selectivities for aqueous-phase dehydration/hydrogenation of 5 wt.% sorbitol at 538 K and 57.6 bar vs. (A) addition of mineral acid (HCl) in feed over Pt/Al_2O_3 [key: pH_{feed} 7 (white), pH_{feed} 3 (grey), and pH_{feed} 2 (black)] and (B) addition of solid acid to Pt/Al_2O_3. [Key: Pt/Al_2O_3 (white), mixture 2: Pt/Al_2O_3 (3.30 g) and SiO_2–Al_2O_3 (0.83 g) (grey), and mixture 1: Pt/Al_2O_3 (1.45 g) and SiO_2–Al_2O_3 (1.11 g) (black). Figure adapted from [18].]

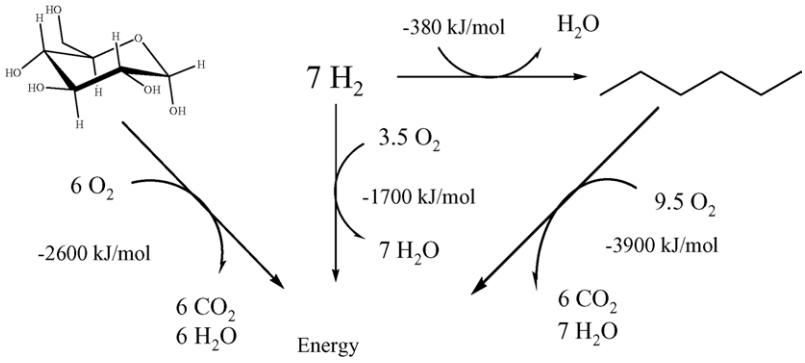

Fig. 9. Energy balance for glucose and H_2 conversion.

could be produced by APR, but H_2 can also be produced by other methods, including solar power, wind power, or nuclear power.

One of the advantages of alkane production from biomass by APD/H is that the alkanes spontaneously separate from the aqueous feed solution, whereas ethanol produced during fermentation processes must be removed from water by an energy-intensive distillation step. Thus, we can compare the overall energy efficiency of alkane production by APD/H with ethanol production, which is the most widely practiced method of producing liquid fuels from biomass. The overall energy efficiency (defined as heating value of ethanol divided by the energy required to produce ethanol from corn) for ethanol production from corn is equal to about 1.1 without co-product energy credits [2]. (During ethanol production a number of other products are made, such as animal feeds, and if energy credits are given for these other products, then the overall energy efficiency increases to 1.3–2.2.) The energy required to produce ethanol from corn (including corn production, corn transportation, ethanol conversion and ethanol transportation) according to Shapouri et al. [2] is 21,525 kJ/$L_{ethanol}$. The total energy required (taking into account the EPA's efficiency factor for the energy used to mine and transport coal) for the ethanol conversion plant is 14,432 kJ/$L_{ethanol}$ [2], of which the actual thermal energy is 10,000 kJ/$L_{ethanol}$. The actual thermal energy (not including the EPA's efficiency factor) required for the distillation process is reported by Katzen et al. to be 5000–5500 kJ/$L_{ethanol}$ [47]; therefore, over half of the energy in the ethanol conversion process is used to distill ethanol from water. If we eliminate the distillation process in ethanol production and assume that the distillation process accounts for 50% of the energy in the ethanol conversion process, then the energy required to produce ethanol from corn would be 14,000 kJ/$L_{ethanol}$. If we use ethanol yields (362 $L_{ethanol}$/$Mg_{biomass}$) and sugar yields (0.82 g_{sugar}/$g_{biomass}$) as reported by Klass [4], then we can estimate that the energy required for conversion of corn to ethanol (excluding distillation) is equal to 6300 kJ/kg_{sugar}; and, we then assume that this value is also equal to the energy required to convert corn to alkanes. Using a value of 2540 kJ/mol for the heat of combustion of glucose and assuming that sugars are converted to alkanes as given by a stoichiometry analogous to Eq. (4), then approximately 96% of the energy of the sugar would be retained in the alkane product, giving a heating value for the alkanes of 13,500 kJ/kg_{sugar}. The overall energy efficiency for conversion of alkanes to corn can now be calculated to be 2.1 by dividing the heating value of the alkanes (13,500 kJ/kg_{sugar}) by the energy required to produce alkanes (6300 kJ/kg_{sugar}). The overall energy efficiency for both conversion of corn to ethanol or corn to alkanes can be increased further by using co-product energy credits [2].

5. Production of liquid alkanes by aqueous-phase processing

5.1. Reaction mechanism

Alkanes produced by the APD/H of carbohydrates would provide a renewable source of transportation fuel to complement the rapidly growing production of bio-diesel from vegetable oils and animal fats [48]. Unfortunately, the largest compound produced by APD/H of carbohydrates is hexane, which has a low value as a fuel additive because of its high volatility [49]. Larger liquid alkanes ranging from C_7 to C_{15} can be produced by first linking carbohydrate-derived moieties through formation of C–C bonds by aldol condensation prior to APD/H processing [19]. It should be noted that the C–O–C linkages (as found in disaccharides) are broken under APD/H reaction conditions.

Aldol condensation is one of the main C–C bond forming reactions. In the first step, a base reacts with the α-H of a carbonyl group to form a carbanion (or enolate) species and water. (When a solid base catalyst is used no water is formed during enolate formation.) The carbanion then reacts with the carbonyl group of an aldehyde to form a new carbon–carbon bond, an alcohol group and regenerating the basic site. Solid or mineral base catalysts can be used to catalyze aldol condensation reactions. Aldol condensation is particularly relevant for the production of large organic compounds from biomass, because various species containing carbonyl groups can be formed from carbohydrates, including furfurals, lactones, dihydroxyacetone, and acetone.

Fig. 10 shows some of the key molecules containing carbonyl groups that can be formed from glucose. Similar molecules can be formed from xylose. While glucose and xylose contain carbonyl groups, they do not undergo aldol-condensation reactions, because the carbonyl group undergoes

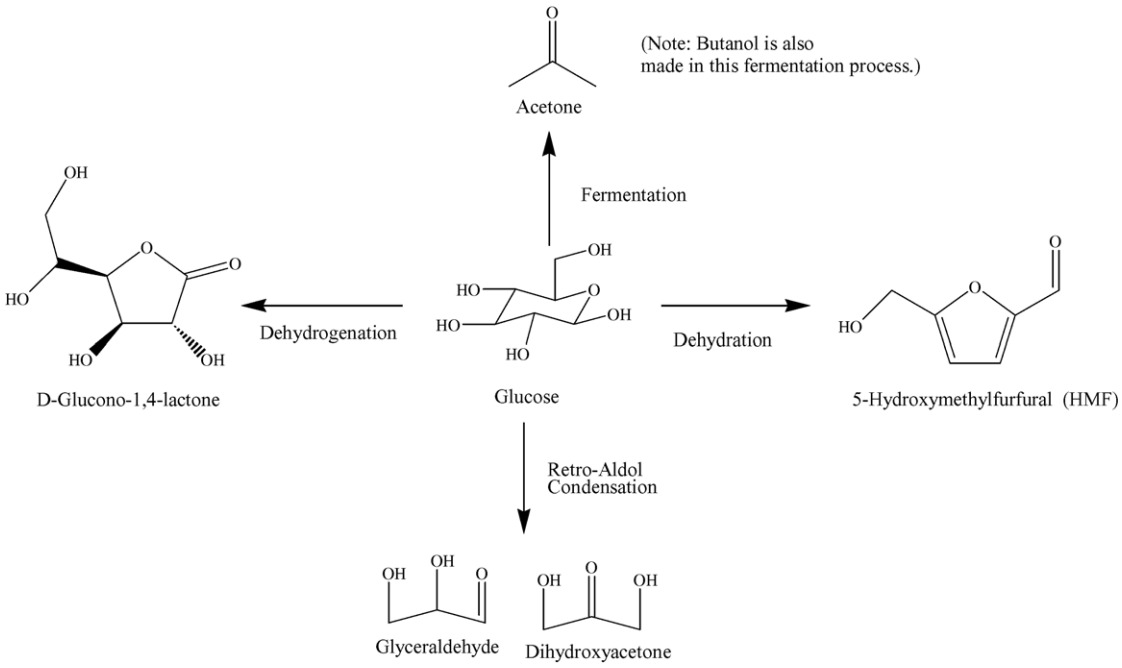

Fig. 10. Routes for formation of chemicals with carbonyl groups from glucose.

intramolecular reactions to form ring structures [50]. However, it is possible to dehydrate glucose and xylose to 5-hydroxymethylfurfural (HMF) and furfural, respectively, using mineral or solid acid catalysts [4,51–54]. Solid acids such as microporous pillared clay catalysts [55], MCM catalysts [55], Y-zeolites [53], mordenite [52], and ZSM-5 [56] have been used to produce HMF from glucose. A selectivity of >90% was achieved for HMF from fructose when mordenite was used as a catalyst and methyl-*iso*-butyl-ketone was added to the aqueous-phase [52]. Similarly, furfural can be produced from xylose over solid acid catalysts with a high selectivity (90–95%) [51].

Both HMF and furfural contain an aldehyde group, and while they cannot undergo self-condensation, because they do not have an α-H atom, they can condense with other molecules that can form carbanion species, such as acetone, dihydroxyacetone or glyceraldehyde. Acetone can be produced from the fermentation of glucose [4], and dihydroxyacetone and glyceraldehyde can be produced from retro-aldol-condensation of glucose [50,57]. Glucose can also be dehydrogenated to form gluconolactone, which contains a carbonyl group [58].

The aldol condensation step can be combined with the dehydration/hydrogenation process to convert carbohydrates to larger alkanes, as described in Fig. 11. In the first step, carbohydrates are dehydrated by acid catalysts, e.g., glucose and xylose are converted to HMF and furfural, respectively. If the C=C bonds of HMF and furfural are selectively hydrogenated (leaving the C=O bond intact), then HMF and furfural are converted to 5-hydroxymethyl-tetrahydrofurfural (HMTHFA) and tetrahydrofuran-2 carboxyaldehyde (THF2A), respectively, which can undergo self-aldol condensation. These large water soluble organic compounds can then be converted to alkanes by dehydration/hydrogenation in a four-phase dehydration/hydrogenation (4PD/H) reactor. Alternatively, HMF and furfural can be condensed with acetone producing large organic compounds ranging from C_8 to C_{15}. These molecules are only slightly water soluble, and must be hydrogenated prior to the final dehydration/hydrogenation to increase their water solubility. In the final dehydration/hydrogenation step, these molecules are converted to straight chain alkanes ranging from C_7 to C_{15}.

The APD/H process described above to convert sorbitol to hexane cannot be used to produce alkanes from large water-soluble organic compounds, because extensive amounts of coke form on the catalyst surface (e.g., 20–50% of the reactant is converted to coke). Accordingly, to produce liquid alkanes the reactor system employed to carry out dehydration/hydrogenation reactions must be modified to a four-phase reactor system (Fig. 12) consisting of (i) an aqueous inlet stream containing the large water-soluble organic reactant, (ii) a hexadecane alkane inlet stream, (iii) a H_2 inlet gas stream, and (iv) a solid catalyst (Pt/SiO_2–Al_2O_3). As dehydration/hydrogenation takes place, the aqueous organic reactants become more hydrophobic, and the hexadecane alkane stream serves to remove hydrophobic species from the catalyst before they react further to form coke. In an industrial setting, the alkanes produced from the reaction would be recycled to the reactor and used for the alkane feed. Reaction kinetic experiments conducted with pure water as the aqueous feed showed that only small amounts of hexadecane were converted to lighter alkanes in the four-phase dehydration/hydrogenation (4-PD/H) reactor system (0.007 μmol min^{-1} g_{cat}^{-1}), and this low reactivity was subtracted from all of our subsequent experimental data.

5.2. Alkane production by aqueous-phase processing

Aldol-condensation of HMF with acetone was carried out with HMF:acetone molar ratios of 1:1 and 1:10 using a mixed

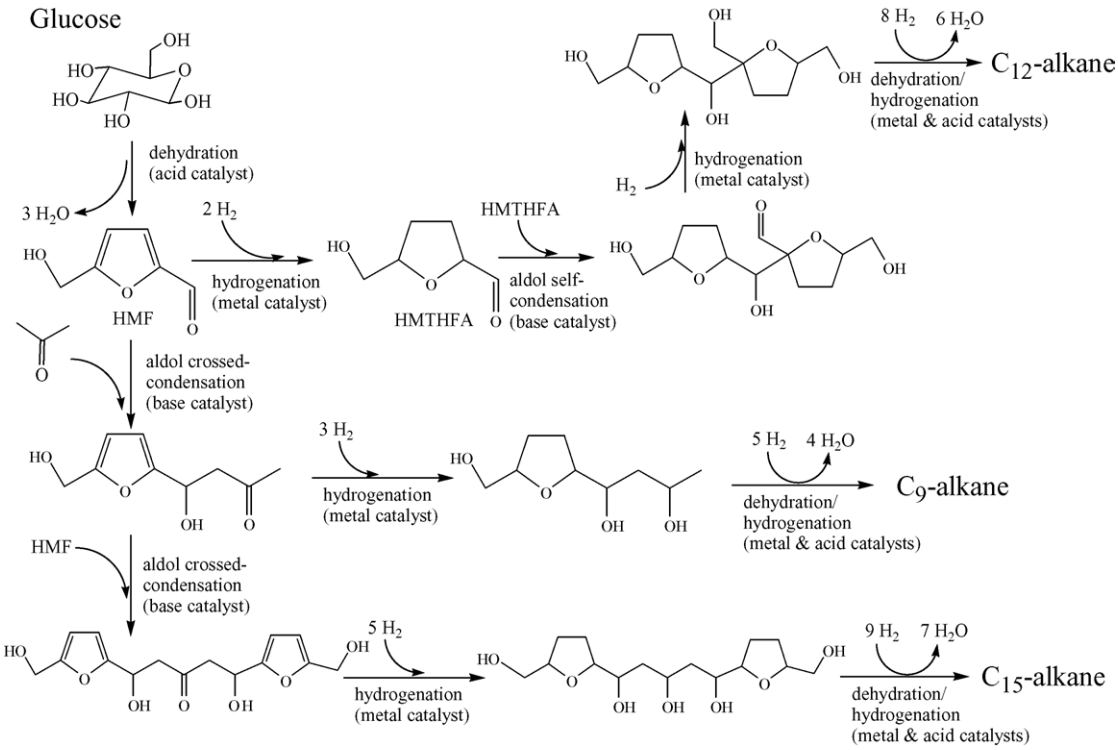

Fig. 11. Reaction pathways for conversion of biomass-derived glucose into liquid alkanes. (Figure adapted from [19].)

Mg–Al-oxide catalyst at room temperature in a batch reactor, as described elsewhere [19]. Aldol-condensation reactions were carried out in water, resulting in formation of insoluble products for HMF:acetone atomic ratios of 1:1. The weight ratio of organic feed to catalyst during condensation was 6 for all feeds except for the HMF:acetone (1:1)-2 (1:1 denotes molar HMF to acetone ratio) feed, which was condensed with an organic feed to catalyst weight ratio of 3. The precipitate formed after condensation was dissolved in excess methanol (a methanol to water weight ratio of 2:1) for the HMF:acetone (1:1)-1 and (1:1)-2, and then hydrogenated in a Parr Reactor with a Pd/Al_2O_3 catalyst to form the water-soluble feed to the 4-PD/H reactor. The water, methanol and acetone were then evaporated and the condensed molecules were re-dissolved in water and converted into alkanes in the 4-PD/H reactor. All other feeds were hydrogenated in water prior to being fed to the 4-PD/H reactor. As shown in Fig. 13, the condensed HMF:acetone products produced mainly C_8 to C_{15} alkanes in the 4-PD/H reactor, depending on the HMF:acetone ratio used in the aldol-condensation step. When the HMF:acetone ratio decreases, the alkane distribution shifts to lighter alkanes. The selectivity can also be shifted to heavier alkanes by increasing the extent of conversion for the aldol condensation step of HMF:acetone, as can be seen comparing the HMF:acetone (1:1)-1 and HMF:acetone (1:1)-2 feeds (Fig. 13).

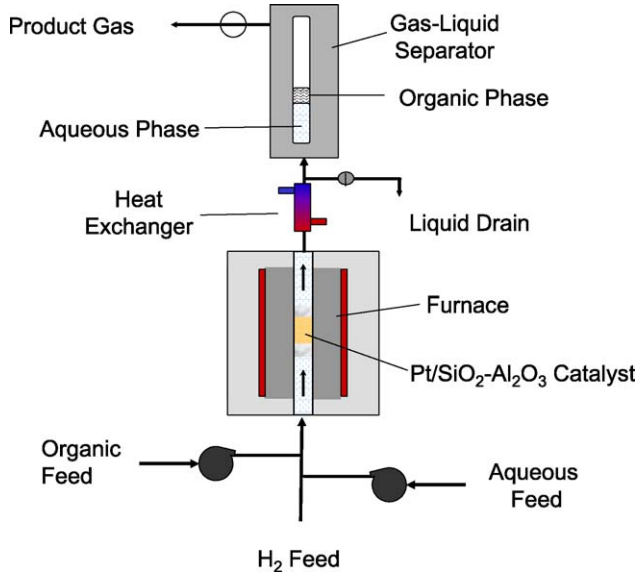

Fig. 12. Schematic diagram of four-phase dehydration/hydrogenation reactor.

To improve the potential practical utility of our process, we studied whether hydrogenation of the HMF:acetone adduct could be accomplished without using methanol as a solvent. For this case, we first carried out the aldol-condensation of HMF:acetone (1:1) in water over the Mg–Al-oxide catalyst, and we then added Pd/Al_2O_3 to the reaction slurry, followed by treatment with H_2 (55 bar) at 393 K in a Parr reactor. We found that hydrogenation of the HMF:acetone adduct increases its solubility in water, and the aqueous solution from this hydrogenation step produced significant amounts of C_{14} and C_{15} alkanes from the 4-PD/H reactor (HMF:Ace-3 in Fig. 13). For this feed a large amount of propane is present in the alkane products, whereas for HMF:acetone (1:1)-1 and HMF: acetone (1:1)-2 no propane is present. The propane is not present for the HMF: acetone (1:1)-1 and HMF: acetone (1:1)-2 feeds because methanol, water and acetone were evaporated from the solution prior to the 4-PD/H step, whereas

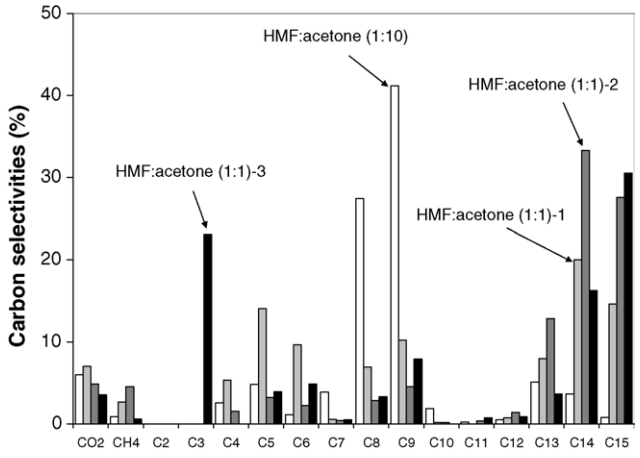

Fig. 13. Carbon selectivities from 4-PD/H processing of cross-condensed HMF:acetone. Legend: HMF:acetone (1:10)—white; HMF:acetone (1:1)-1—light grey; HMF:actone (1:1)-2—dark grey; and HMF:acetone (1:1)-3—black. [Key: HMF:acetone (1:1)-1 and HMF:acetone (1:1)-2 were condensed in H_2O and then hydrogenated in mixtures of methanol and water. HMF:acetone (1:1)-2 was condensed with twice the amount of catalyst as HMF:acetone (1:1)-1. HMF:acetone (1:10) and HMF:acetone (1:1)-3 were condensed and hydrogenated in water. Propane is not included in the selectivity calculation for the HMF:acetone (1:10) feed. For detailed reaction conditions see [19].]

no evaporation step was used with the HMF: acetone (1:1)-3 feed. Thus, in the condensation of HMF with acetone, 23% of the carbon is unreacted acetone and future research should focus on how to use the remaining acetone. Propane is also not included in the selectivity calculation for the HMF:acetone (1:10) feed.

Mixtures of HMF and furfural (HMF:furfural:acetone (1:1:2)) can also be condensed with acetone to form alkanes ranging from *n*-C_7 to C_{15}, as shown in Fig. 14. This mixture was condensed with a Mg–Al-oxide catalyst at room temperature and then hydrogenated with a Pd/Al_2O_3 catalyst in the aqueous phase. This result shows that, unlike for the production of ethanol by fermentation, cellulose and hemicellulose do not need to be separated for effective production of liquid alkanes by 4-PD/H processing. Aqueous-phase aldol condensation reactions have previously been carried out with glyceraldehyde,

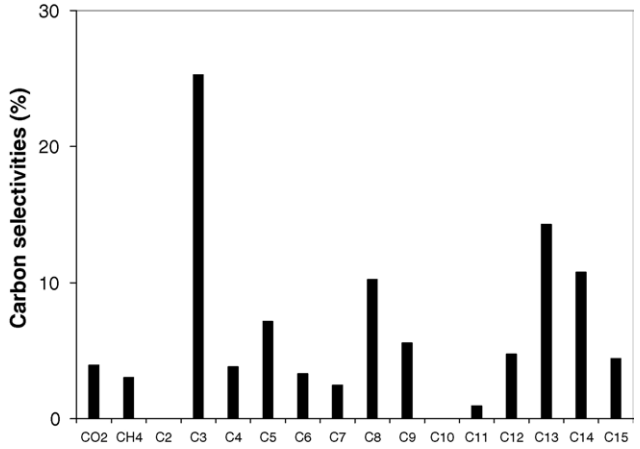

Fig. 14. Carbon selectivities from 4-PD/H processing of cross-condensed HMF:Furfural:acetone (1:1:2). (For reaction conditions see [19].)

dihydroxyacetone, formaldehyde and butyraldehyde using both homogeneous and heterogeneous base catalysts [59,60]. Cross-condensation of furfural with acetone has been conducted using amino-functionalized mesoporous base catalysts [61]. Mixed Mg–Al-oxides have previously been used as solid base catalysts for liquid-phase aldol condensation reactions [62,63].

Results for crossed aldol-condensation of furfural and HMF with dihydroxyacetone over Mg–Al-oxide catalyst showed a large disappearance of furfural and HMF based on HPLC; however, less than 30% of the alkane products are heavier than the C_5 and C_6 reactants for reactions of furfural and HMF, respectively [19]. Changing the molar furfural to dihydroxyacetone ratio did not significantly improve the selectivity to heavier alkanes. Condensing furfural with hydroxyacetone or glyceraldehyde gave an alkane distribution similar to that produced from condensation of furfural with dihydroxyacetone. These results show that it is possible to make heavier liquid alkanes by crossed aldol-condensation of furfural and HMF with dihydroxyacetone, hydroxyacetone, or glyceraldehydes; however, it will be necessary to improve the selectivities of these processes.

Another route to make large water-soluble organic compounds is to selectively hydrogenate the C=C bonds of HMF and furfural, producing 5-hydroxymethyl-tetrahydrofurfural (HMTHFA) and tetrahydrofuran-2 carboxyaldehyde (THF2A), respectively. These species can form carbanion species and undergo self-aldol-condensation reactions (Fig. 11). Self-aldol-condensation of THF2A produced liquid hydrocarbons ranging from C_8 to C_{10} from the 4-PD/H reactor. Tetrahydrofurfural-2-aldehyde (THF2A) was prepared by selective dehydrogenation of tetrahydrofurfural alcohol (Aldrich) in a gas-phase fixed-bed reactor using a 10 wt.% Cu/SiO_2 catalyst (Cab-o-sil), prepared by incipient wetness impregnation [64].

6. Biorefinery for a carbohydrate-based economy

Fig. 15 shows a proposed biorefinery for converting biomass into liquid alkanes based on aqueous-phase processing. In the first step, cellulose and hemicellulose are respectively converted to xylose and glucose. Part of the sugar stream is then converted to H_2 by APR for use elsewhere in the plant. Furfural and HMF are produced from the remaining sugar stream by acid-catalyzed dehydration. Furfural and HMF are then condensed with acetone over a solid base catalysts to produce large water soluble organic compounds. In the final reactor, a four-phase dehydration/hydrogenation unit (4-PD/H), the condensed products are dehydrated and hydrogenated to produce large liquid alkanes (ranging from C_7 to C_{15}) over a bifunctional catalyst containing metal and acid sites.

While our initial results show that these processes are indeed technically feasible, it is likely that future advances will further optimize these processes, thus providing a transition from a petroleum-based economy to a carbohydrate-based economy.

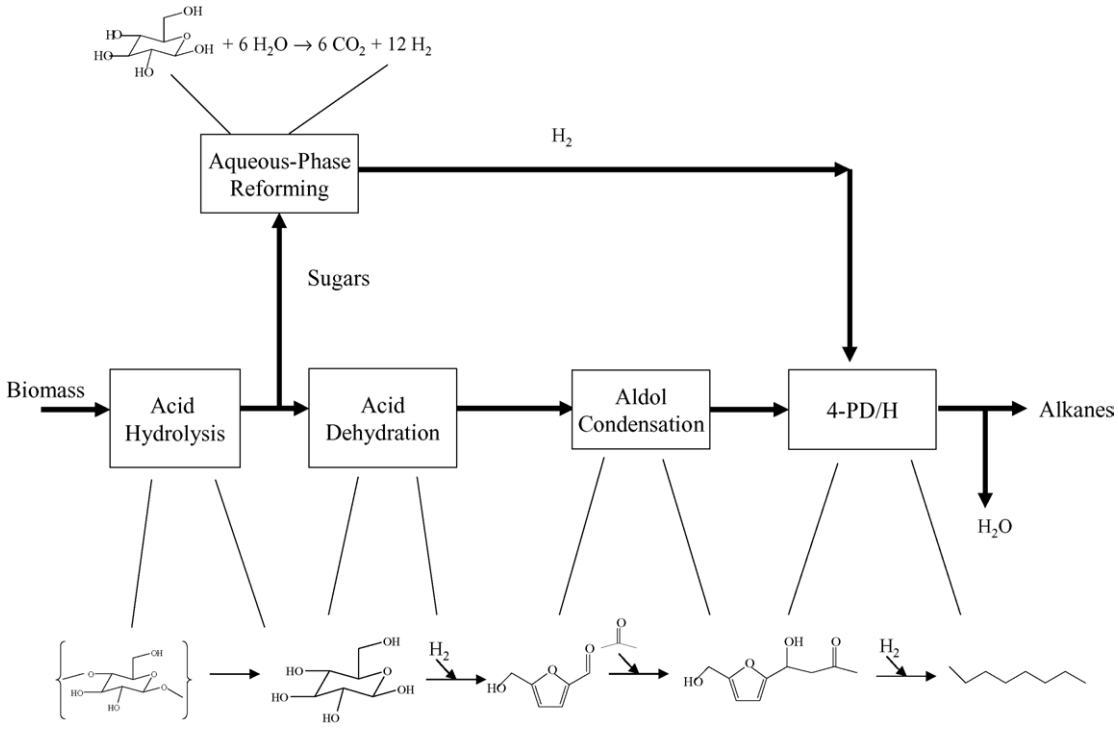

Fig. 15. Self-sustaining biomass-refinery for conversion of biomass into liquid alkanes using aqueous-phase processing.

7. Summary

Aqueous-phase processing is a promising option for conversion of biomass into fuels including H_2 and alkanes ranging from C_1 to C_{15}. An effective catalyst for the production of H_2 from APR should be active for C–C bond cleavage and water-gas shift. Importantly, the catalyst must not facilitate the subsequent methanation and/or Fischer–Tropsch synthesis reactions to produce alkanes, which consume H_2. Catalysts for production of H_2 should also have low rates of C–O bond cleavage to form alkane products. From our reaction kinetics studies, we have found that Pt is the best monometallic catalyst in terms of activity and selectivity for APR. We have identified several bimetallic catalysts, including PtNi, PtCo, PtFe and PdFe which have higher activities than monometallic catalysts. While Ni catalysts are active for APR, they produce a large amount of methane, and these catalyst exhibit deactivation. The amount of methane can be decreased by alloying the Ni with Sn. The stability of Ni-based catalysts can be improved by using a Raney-Ni catalyst. Accordingly, a Raney-NiSn catalyst can be used to achieve good activity, selectivity, and stability for production of H_2 by APR of biomass-derived oxygenated hydrocarbons.

A stream of alkanes ranging from C_1 to C_6 can be formed by aqueous-phase dehydration/hydrogenation (APD/H) of sorbitol over bi-functional catalyst systems in which sorbitol is repeatedly dehydrated by an acid catalyst (e.g., a solid acid or an aqueous mineral acid) and then hydrogenated on a metal catalyst (e.g., Pt or Pd). Hydrogen, which is needed for the hydrogenation reaction, can be produced in-situ by APR of sorbitol over a catalyst (such as Pt) that facilitates C–C bond cleavage and water-gas shift reactions, or it can be co-fed to the reactor with the aqueous sorbitol reactant.

Liquid alkanes ranging from C_7 to C_{15} can be produced from carbohydrates by combining the dehydration/hydrogenation process with an aldol condensation step to form C–C bonds. Biomass-derived compounds, such as furfural, HMF and acetone, that contain carbonyl groups, were coupled by aldol condensation at room temperature using a mixed Mg–Al-oxide base catalyst to form large organic molecules. The reaction mixtures were then hydrogenated, using a 5% Pd/Al_2O_3 catalyst, to increase the aqueous solubility of these molecules and to minimize possible coking reactions that may take place from unsaturated molecules in the following step. The hydrogenated molecules were subsequently converted to alkanes by dehydration/hydrogenation over a bi-functional catalyst (4 wt.% Pt/SiO_2–Al_2O_3) containing acid and metal sites in a specially designed four-phase reactor system. This reactor system consists of an aqueous inlet stream containing the large water-soluble organic reactant, a hexadecane alkane sweep stream, a H_2 inlet gas stream, and a solid catalyst. During dehydration/hydrogenation processing, organic species are transferred from the aqueous phase reactant stream to the hexadecane sweep stream as these organic species become more hydrophobic, removing these species from the catalyst as valuable products before they go on further to form coke.

Acknowledgements

This work was supported by the U.S. Department of Energy (DOE) Office of Basic Energy Sciences, and the National Science Foundation (NSF) Chemical and Transport Systems

Division of the Directorate for Engineering. We would like to thank John W. Shabaker, Rupali R. Davda, Randy D. Cortright, Juben N. Chheda and Chris J. Barrett for their invaluable collaborations during all phases of this work.

References

[1] L.R. Lynd, C.E. Wyman, T.U. Gerngross, Biotechnol. Prog. 15 (1999) 777.
[2] H. Shapouri, J.A. Duffield, M. Wang, The Energy Balance of Corn: An Update, No. 814, U.S. Department of Agriculture, Office of the Chief Economist, 2002. http://www.usda.gov/oce/oepnu/aer-814.pdf.
[3] Biomass Research and Development Technical Advisory Committee, Roadmap for Biomass Technologies in the U.S., U.S. Government, 2002. http://www.bioproducts-bioenergy.gov/pdfs/Final Biomass Roadmap.pdf.
[4] D.L. Klass, Biomass for Renewable Energy, Fuels and Chemicals, Academic Press, San Diego, 1998.
[5] Energy Information Administration, Annual Energy Outlook 2004, U.S. Department of Energy, DOE/EIA-0383, 2004. http://www.eia.doe.gov/oiaf/aeo/.
[6] R.D. Perlack, L.L. Wright, A. Turhollow, R.L. Graham, B. Stokes, D.C. Erbach, Biomass as Feedstock for a Bioenergy and Bioproducts Industry: The Technical Feasibility of a Billion-Ton Annual Supply, Oak Ridge National Laboratory, 2005 DOE/GO-102995-2135. http://www.osti.gov/bridge.
[7] R.D. Cortright, R.R. Davda, J.A. Dumesic, Nature 418 (2002) 964.
[8] R.R. Davda, J.A. Dumesic, Angew. Chem. Int. Ed. 42 (2003) 4068.
[9] R.R. Davda, J.W. Shabaker, G.W. Huber, R.D. Cortright, J.A. Dumesic, Appl. Catal. B 43 (2003) 1.
[10] R.R. Davda, J.W. Shabaker, G.W. Huber, R.D. Cortright, J.A. Dumesic, Appl. Catal. B 56 (2005) 171.
[11] G.W. Huber, J.W. Shabaker, S.T. Evans, J.A. Dumesic, Appl. Catal. B, in press.
[12] G.W. Huber, J.W. Shabaker, J.A. Dumesic, Science 300 (2003) 2075.
[13] J.W. Shabaker, R.R. Davda, G.W. Huber, R.D. Cortright, J.A. Dumesic, J. Catal. 215 (2003) 344.
[14] J.W. Shabaker, J.A. Dumesic, Ind. Eng. Chem. Res. 43 (2004) 3105.
[15] J.W. Shabaker, G.W. Huber, R.R. Davda, R.D. Cortright, J.A. Dumesic, Catal. Lett. 88 (2003) 1.
[16] J.W. Shabaker, G.W. Huber, J.A. Dumesic, J. Catal. 222 (2004) 180.
[17] J.W. Shabaker, D.A. Simonetti, R.D. Cortright, J.A. Dumesic, J. Catal. 231 (2005) 67.
[18] G.W. Huber, R.D. Cortright, J.A. Dumesic, Angew. Chem. Int. Ed. 43 (2004) 1549.
[19] G.W. Huber, J.N. Chheda, C.J. Barrett, J.A. Dumesic, Science 308 (2005) 1446.
[20] C.E. Wyman, Annu. Rev. Energy Environ. 24 (1999) 189.
[21] U.S. Department of Energy, Feedstock Composition Glossary, U.S. Department of Energy, 2005. http://www.eere.energy.gov/biomass/feedstock_glossary.html.
[22] Y. Sun, J. Cheng, Bioresour. Technol. 83 (2002) 1.
[23] N. Mosier, C. Wyman, B. Dale, R. Elander, Y.Y. Lee, M. Holtzapple, M. Ladisch, Bioresour. Technol. 96 (2005) 673.
[24] A. Aden, M. Ruth, K. Ibsen, J. Jechura, K. Neeves, J. Sheehan, B. Wallace, L. Montague, A. Slayton, J. Lukas, Lignocellulosic Biomass to Ethanol Process Design and Economics Utilizing Co-Current Dilute Acid Prehydrolysis and Enzymatic Hydrolysis for Corn Stover, National Renewable Energy Laboratory, 2002 NREL/TP-510-32438.
[25] E. Berl, Science 99 (1944) 309.
[26] D.C. Elliott, D. Beckman, A.V. Bridgwater, J.P. Diebold, S.B. Gevert, Y. Solantausta, Energy Fuels 5 (1991) 399.
[27] P.B. Weisz, W.O. Haag, P.G. Rodewald, Science 206 (1979) 57.
[28] N.Y. Chen, J.T.F. Degnan, L.R. Koenig, Chem. Technol. 16 (1986) 506.
[29] H. Heinemann, Petrol. Refiner 33 (1954) 161.
[30] H. Heinemann, Petrol. Refiner 33 (1954) 135.
[31] D.J. Wilhelm, D.R. Simbeck, A.D. Karp, R.L. Dickenson, Fuel Process. Technol. 71 (2001) 139.
[32] R.W.R. Zwart, H. Boerrigter, Energy Fuels 19 (2005) 591.
[33] R.J. Farrauto, C.H. Bartholomew, Introduction to Industrial Catalytic Processes, Chapman & Hall, London, UK, 1997.
[34] R.P. Datar, R.M. Shenkman, B.G. Cateni, R.L. Huhnke, R.S. Lewis, Biotechnol. Bioeng. 86 (2004) 587.
[35] H. Boerrigter, 'Green' Diesel Production with Fischer–Tropsch Synthesis, ECN Biomass, ECN-RX-03-014, 2003. http://www.ecn.nl/_files/bio/RX03014.pdf.
[36] M.J. Prins, K.J. Ptasinski, F.J.J.G. Janssen, Fuel Process. Technol. 86 (2004) 375.
[37] M. Mavrikakis, M.A. Barteau, J. Mol. Catal. A: Chem. 131 (1998) 135.
[38] J.F.E. Gootzen, W. Visscher, J.A.R. van Veen, Langmuir 12 (1996) 5076.
[39] J.F.E. Gootzen, A.H. Wonders, W. Visscher, J.A.R. van Veen, Langmuir 13 (1997) 1659.
[40] R. He, R.R. Davda, J.A. Dumesic, J. Phys. Chem. B 109 (2005) 2810.
[41] A.V. Ruban, H.L. Skriver, J.K. Norskov, Phys. Rev. B: Condens. Matter 59 (1999) 15990.
[42] E. Christoffersen, P. Liu, A. Ruban, H.L. Skriver, J.K. Norskov, J. Catal. 199 (2001) 123.
[43] J.R. Kitchin, J.K. Norskov, M.A. Barteau, J.G. Chen, J. Chem. Phys. 120 (2004) 10240.
[44] J. Greeley, M. Mavrikakis, Nat. Mater. 3 (2004) 810.
[45] P. Stoss, R. Hemmer, Adv. Carbohydr. Chem. Biochem. 49 (1991) 93.
[46] J.A. Dean, Lange's Handbook of Chemistry, McGraw-Hill, New York, 1999.
[47] R. Katzen, W.R. Ackley, G.D. Moon Jr., J.R. Messick, B.F. Brush, K.F. Kaupisch, in: D.L. Klass, G.H. Emert (Eds.), Fuels from Biomass and Wastes, Ann Arbor Science, Ann Arbor, MI, 1981, p. 393.
[48] F. Ma, M.A. Hanna, Bioresour. Technol. 70 (1999) 1.
[49] K. Owen, T. Coley, Automotive Fuels Handbook, Society of Automotive Engineers, Warrendale, PA, 1990.
[50] P. Collins, R. Ferrier, Monosaccharides, Wiley, West Sussex, UK, 1995.
[51] C. Moreau, R. Durand, D. Peyron, J. Duhamet, P. Rivalier, Ind. Crop. Prod. 7 (1998) 95.
[52] C. Moreau, R. Durand, S. Razigade, J. Duhamet, P. Faugeras, P. Rivalier, P. Ros, G. Avignon, Appl. Catal. A 145 (1996) 211.
[53] K. Lourvanij, G.L. Rorrer, Ind. Eng. Chem. Res. 32 (1993) 11.
[54] J. Lewkowski, ARKIVOC, Part (i) (2001) 17.
[55] K. Lourvanij, G.L. Rorrer, Appl. Catal. A 109 (1994) 147.
[56] P. Rivalier, J. Duhamet, C. Moreau, R. Durand, Catal. Today 24 (1995) 165.
[57] M. Sasaki, K. Goto, K. Tajima, T. Adschiri, K. Arai, Green Chem. 4 (2002) 285.
[58] M. Bierenstiel, M. Schlaf, Eur. J. Org. Chem. 2004 (2004) 1474.
[59] C.D. Gutsche, D. Redmore, R.S. Buriks, K.A. Nowotny, H. Grassner, C.W. Armbruster, J. Am. Chem. Soc. 89 (1967) 1235.
[60] V. Serra-Holm, T. Salmi, J. Multamäki, J. Reinik, P. Mäki-Arvela, R. Sjöholm, L.P. Lindfors, Appl. Catal. A 198 (2000) 207.
[61] B.M. Choudary, M. Lakshmi Kantam, P. Sreekanth, T. Bandopadhyay, F. Figueras, A. Tuel, J. Mol. Catal. A 142 (1999) 361.
[62] M.J. Climent, A. Corma, S. Iborra, K. Epping, A. Velty, J. Catal. 225 (2004) 316.
[63] K.K. Rao, M. Gravelle, J.S. Valente, F. Figueras, J. Catal. 173 (1998) 115.
[64] R.D. Cortright, M. Sanchez-Castillo, J.A. Dumesic, Appl. Catal. B 39 (2002) 353.